Electromagnetic Absorption in Multilayered Cylindrical Models of Man

HABIB MASSOUDI, MEMBER, IEEE, CARL H. DURNEY, MEMBER, IEEE, PETER W. BARBER, MEMBER, IEEE, AND MAGDY F. ISKANDER, MEMBER, IEEE

Abstract—**The absorption characteristics of multilayered cylindrical models of man irradiated by a normally incident electromagnetic plane wave are investigated. Numerical calculations for a specific skin-fat-muscle cylindrical model of man predict a layering resonance at 1.2 GHz with an average specific absorption rate (SAR) about double that calculated for the corresponding homogeneous model. The layering resonance frequency is found to be the same for incident waves polarized parallel and perpendicular to the cylinder axis. The effects of layers on whole-body absorption by man are determined by averaging the effects obtained for many combinations of skin and fat thicknesses. Absorption effects due to clothing are also investigated.**

I. Introduction

THE absorption characteristics of multilayered spherical models of the human head exposed to electromagnetic (EM) plane waves have been investigated by Joines and Spiegel [1] and by Weil [2]. They have shown that there is a layering resonance in the specific absorption rate (SAR) versus frequency curve for the multilayered spherical model that occurs at frequencies higher than the geometrical resonance. The SAR is the average absorption in watts per kilogram or milliwatts per cubic centimeter (assuming a tissue density of 1 g/cm^3). A multilayered planar model has recently been utilized by Barber *et al.* [3] to examine the dependence of whole-body power absorption on the configuration of surface layers. They found the following.

1) A planar model can accurately predict the layering resonance frequencies for a nonplanar geometry.

2) The resonance due to the gross geometry of the body and the resonance due to the layers are independent of one another if the layers are a small fraction of the maximum dimension.

3) Calculations for a multilayered planar model of an average man predict a whole-body layering resonance at 1.8 GHz with a SAR 34 percent greater than that predicted by a homogeneous model.

Since the layering effect appears to be significant, and since it occurs in the frequency range where a cylindrical model gives good results for the homogeneous case [4], the effect of skin-fat-muscle layering, as well as the effect of clothing, on the average SAR in a multilayered cylindrical model of man have been investigated and the results are presented in this paper.

Manuscript received January 9, 1979; revised April 30, 1979. This work was supported by the USAF School of Aerospace Medicine, Brooks Air Force Base, under Contract F41609-76-C-0025/P00004.

The authors are with the Departments of Electrical Engineering and Bioengineering, University of Utah, Salt Lake City, UT 84112.

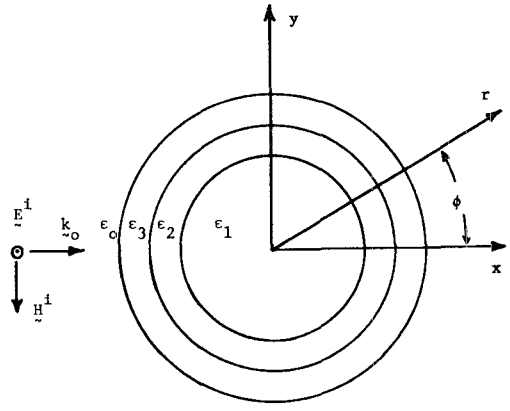

Fig. 1. An electromagnetic plane wave incident upon a multilayered lossy circular cylinder.

II. Formulation

Consider an EM plane wave incident normally on an infinitely long multilayered circular cylinder. The coordinate system with respect to the cylinder is oriented as shown in Fig. 1. The x axis is the axis of propagation of the incident plane wave. Let the cylinder consist of m lossy homogeneous layers, each layer being a circular cylindrical shell. The complex permittivity of layer m is denoted by $\epsilon_m = \epsilon'_m - j\epsilon''_m$, and the permeability of each layer is assumed to be equal to that of free space μ_0.

The average SAR is calculated for the following two different polarizations.

1) The incident E-field parallel to the axis (E-polarization).

2) The incident H-field parallel to the axis (H-polarization).

For the case of E-polarization, the expressions for electric field outside the cylinder E_z and the electric field inside each layer E_{zm} are given as [5]

$$E_z = E_0 e^{j\omega t} \sum_{n=0}^{\infty} \left[e_n j^{-n} J_n(k_0 r) + C_n H_n^{(2)}(k_0 r) \right] \cos n\phi \quad (1)$$

$$E_{z,m} = E_0 e^{j\omega t} \sum_{n=0}^{\infty} \left[A_{mn} J_n(k_m r) + B_{mn} Y_n(k_m r) \right] \cos n\phi \quad (2)$$

0018-9480/79/1000-0825$00.75 ©1979 IEEE

and the magnetic field in each layer is

$$H_{\phi,m} = \frac{1}{j\omega\mu_0}\frac{\partial}{\partial r}E_{z,m} \tag{3}$$

where

E_0 peak value of the incident electric field,
k_0 $2\pi f/c$,
k_m $k_0\sqrt{\epsilon_m}$,
f frequency,
j $(-1)^{1/2}$,
c velocity of light in vacuum,

$$e_n = \begin{cases} 1, & \text{for } n=0 \\ 2, & \text{for } n>0. \end{cases}$$

$J_n(x)$ and $Y_n(x)$ are the cylindrical Bessel functions of the first and the second kind, respectively, and $H_n^{(2)}(x)$ is the Hankel function of the second kind. The unknown coefficients A_{mn}, B_{mn}, and C_n can be determined by matching $E_{z,m}$ and $H_{\phi,m}$ across each cylindrical boundary. For a cylinder consisting of m layers, a set of $2m$ simultaneous equations with $2m$ unknowns must be solved; i.e., the inversion of a $2m$ square matrix with complex elements is to be performed. However, Bussey and Richmond [5] have used a recursion method for calculating the scattering amplitude of a lossy multilayered cylinder, thus avoiding the necessity of inverting the complex matrix. Their technique is applied here for calculating the average SAR in the multilayered cylindrical model of man, as outlined below. The calculated scattered far field, using the asymptotic form of the Hankel function, is

$$E^s = E_0(2j/\pi k_0 r)^{1/2} e^{j(\omega t - k_0 r)} \sum_{n=0}^{\infty} e_n D_n \cos n\phi \tag{4}$$

with

$$D_n = j^n C_n / e_n. \tag{5}$$

The scattering amplitude is given by [6]

$$T(\phi) = \sum_{n=0}^{\infty} e_n D_n \cos n\phi. \tag{6}$$

From (6), the extinction and scattering efficiencies are obtained as [6]

$$Q_{\text{ext}} = \frac{2}{k_0 a}\text{Re}\{T(0)\} \tag{7}$$

$$Q_{\text{sca}} = \frac{1}{\pi k_0 a}\int_0^{2\pi} |T(\phi)|^2 d\phi \tag{8}$$

where a is the outside radius of the cylinder. The absorption efficiency is the difference between the extinction and scattering efficiencies. Using (6)–(8), the absorption efficiency for the cylinder is determined as

$$Q_{\text{abs}} = Q_{\text{ext}} - Q_{\text{sca}} = \frac{2}{k_0 a}\left\{\text{Re}\left[\sum_{n=0}^{\infty} e_n D_n\right] - \sum_{n=0}^{\infty} e_n |D_n|^2\right\}. \tag{9}$$

The absorption efficiency is also defined as the total power absorbed (average SAR × volume) divided by the power incident on the geometrical cross section. From this definition and using (9), the average SAR for an incident power density of 1 mW/cm^2 in the cylindrical model is

$$\text{SAR} = \frac{2Q_{\text{abs}}}{\pi a}, \quad \text{mW/cm}^3 \tag{10}$$

where a is given in centimeters. The above relation holds both for E- and H- polarizations. In the numerical calculations that follow, the frequency dependent complex permittivity of the various tissue types is taken from [7].

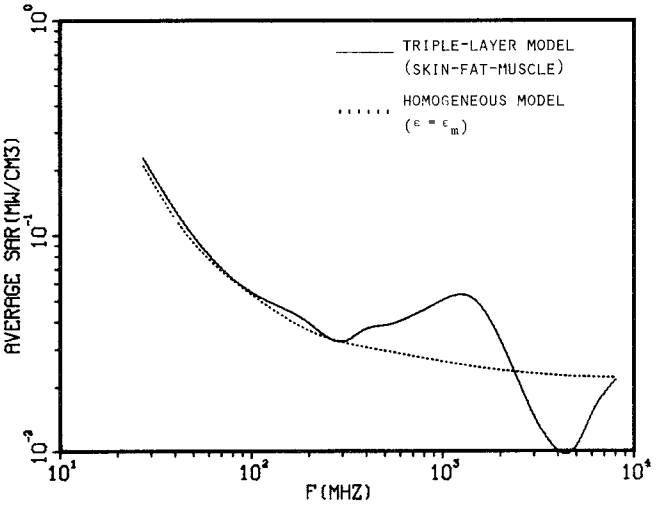

Fig. 2. Average SAR in a triple-layer cylindrical model of an average man, E-polarization. The two outside layers (and thickness) are skin (0.2 cm), fat (1 cm). The radius of the inner muscle cylinder is 10.08 cm. The incident power density is 1 mW/cm^2.

III. Effects of Layers on Absorption

The surface layers of man generally consist of skin-fat-muscle or skin-fat-muscle-bone-muscle arrangements. SAR results for a triple layer skin-fat-muscle cylindrical model of an average man are compared to a homogeneous muscle tissue model for E-polarization in Fig. 2. The layering has caused a significant effect on the average SAR as compared to the homogeneous results. For this three-layered model with 2-mm skin and 1-cm fat thicknesses, the average SAR is increased by 108 percent at 1.2 GHz and reduced by 55 percent at 4.5 GHz. Similar results have been obtained for a semi-infinite planar model with the same skin and fat thicknesses as in our cylindrical model [Barber, unpublished report]. The results shown in Fig. 2 support the idea of Barber *et al.* [3] that the layering resonance is independent of the gross geometry of the absorber.

Fig. 3 shows the average SAR for the triple-layer and homogeneous models for H-polarization. Note that the average SAR is increased by 53 percent at 1.3 GHz and reduced by 58 percent at 4.5 GHz, compared to the muscle cylinder. It is also interesting to note that the resonance due to layering for both polarizations occurs at the same frequency, suggesting that the frequency of the layering resonance is independent of the polarization.

The dependence of the absorption resonance on skin and fat thicknesses for a triple-layered cylindrical model

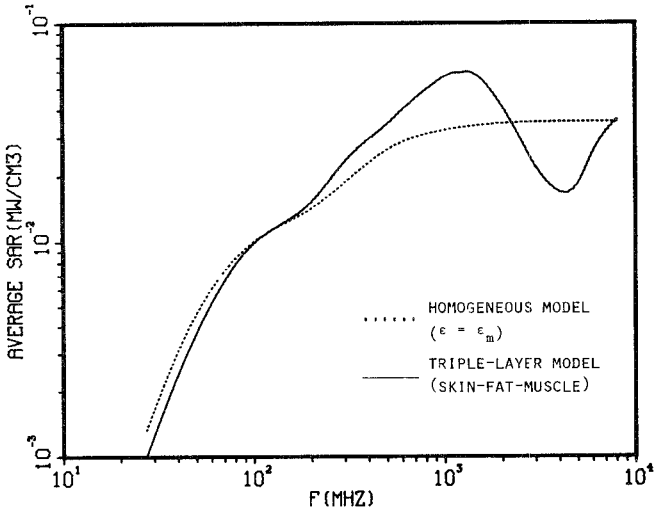

Fig. 3. Average SAR in a triple-layer cylindrical model of an average man, *H*-polarization. The layers are the same as those in Fig. 2. The incident power density is 1 mW/cm^2.

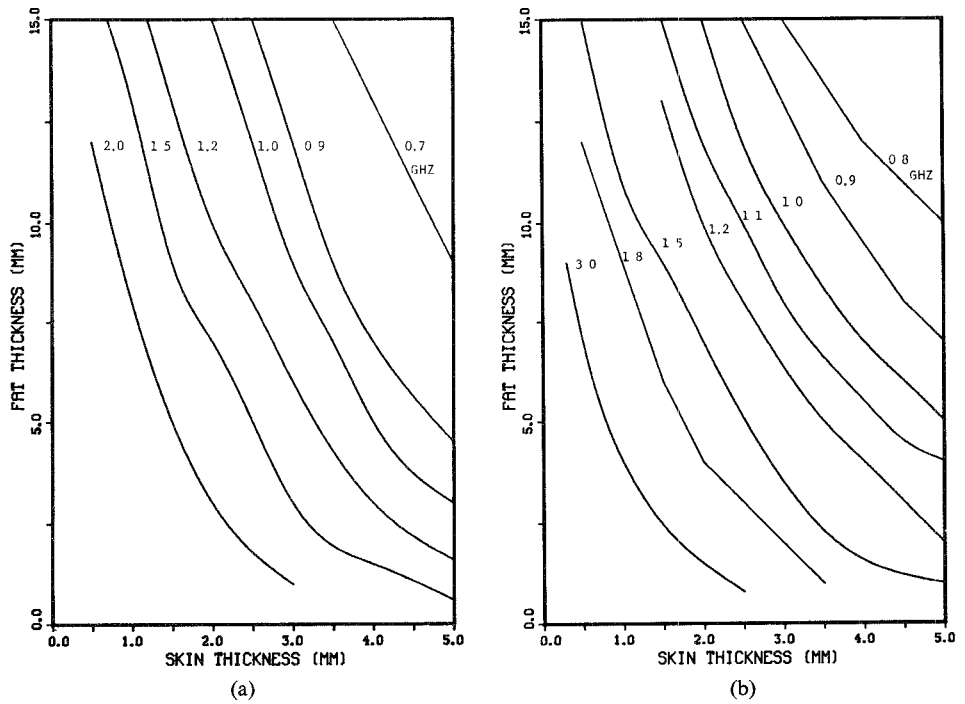

Fig. 4(a). Layering resonance frequency as a function of skin and fat thicknesses for a skin-fat-muscle cylindrical model of man, *E*-polarization. The outer radius of the cylinder is 11.28 cm. (b) Layering resonance frequency as a function of skin and fat thicknesses for a skin-fat-muscle cylindrical model of man, *H*-polarization. The outer radius of the cylinder is 11.28 cm.

of an average man with a skin-fat-muscle arrangement has been investigated numerically by making calculations for all combinations of normally occurring [8], [9] skin and fat thicknesses. The resonance frequency as a function of skin and fat thickness for *E*-polarization is shown in Fig. 4(a). Fig. 4(b) illustrates similar results for *H*-polarization. For both *E*- and *H*-polarizations it can be seen from Fig. 4(a) and (b) that the resonance frequency is inversely proportional to the thickness of layers. The resonance frequency increases as either or both layer thicknesses decrease. Although it seems clear that the resonance effect is caused by an interference-like phenomenon in the layers, we have not been able to identify a simple relationship between layer thickness and wavelength (such as some combination of thicknesses related to a half-wavelength) that will explain the resonance.

IV. Effects of Layers on Whole-Body SAR in Man

In order to study the effects of layers on the whole-body absorption characteristics of man, tissue thicknesses were examined in 52 horizontal cross sections of a standing man. For example, each arm was represented by a combination of eight short-layered cylinders, each cylinder having a different combination of layers of bone, muscle, fat, and skin. The thickness of each layer was estimated from published data on anatomical cross sections [8], [9]. Average thickness of the layers of skin, fat, muscle, and bone were calculated over each cross section. Calculations of the average SAR were made for each of the 52 layered cylinders. Then the average SAR for the whole body was obtained from the following expression:

$$\text{SAR} = \left(\sum_{i=1}^{N} (\text{SAR})_i v_i \right) \Big/ \sum_{i=1}^{N} v_i$$

where $N = 52$ and v_i is the volume of each cylinder. In these calculations, the SAR in each short-layered cylinder was calculated as though each cylinder were infinitely long. This neglects, of course, the coupling between cylinders. However, at high-enough frequencies, this would be a reasonable approximation. At lower frequencies, though, the approximation would not be valid. Thus in the data presented, care should be taken in interpreting the results, especially at the lower frequencies. The lowest applicable frequency for a cylindrical model of an average man has been determined to be 400 MHz [4]. The solid curve in Fig. 5 represents the whole-body average SAR for E-polarization. The dashed curve in Fig. 5 represents the average SAR in a layered cylindrical model of man consisting of six cylinders. For this model each part of the body (arms, legs, head, and torso) was represented by a single-layered cylinder. The dotted curve represents the average SAR for the homogeneous model consisting of six cylinders.

It can be seen from Fig. 5 that the average SAR in the layered cylindrical model with 52 cylinders is nearly the same as that of the layered cylindrical model with six cylinders. Note that the averaging over many cylinders has diminished somewhat the strong peaks that occur in a single-layered cylinder (Fig. 2). However, there is still an absorption enhancement over homogeneous muscle tissue of 44 percent at 1 GHz and a reduction of 50 percent at 5 GHz. Furthermore, comparison of the solid curves in Figs. 2 and 5 shows that for frequencies above 400 MHz, the average SAR in the model consisting of 52 cylinders is about 60 percent higher than that of the triple-layer model. This difference in the SAR values in the two models is caused by differences in the shadow area of the models with respect to the incident wave.

The results of the foregoing analysis have been used to modify previous SAR calculations that have been obtained for homogeneous models of man. Fig. 6 shows the

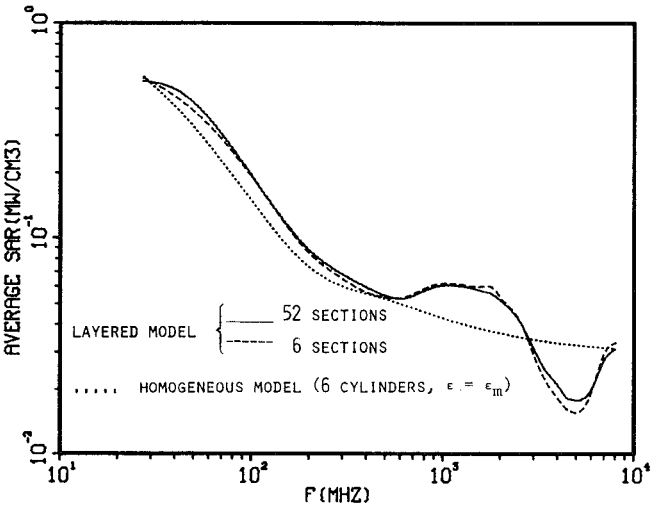

Fig. 5. Average SAR characteristics of the multilayer cylindrical model of man consisting of several cross sections, E-polarization. The incident power density is 1 mW/cm^2.

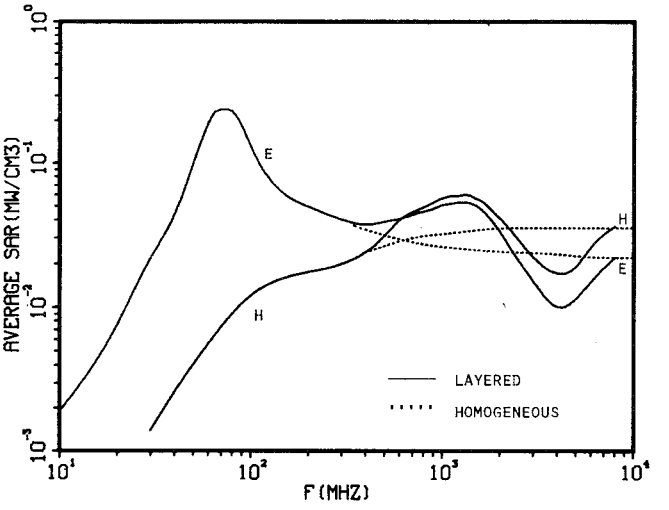

Fig. 6. Average SAR in homogeneous and multilayered models of an average man for an incident power density of 1 mW/cm^2 for two polarizations.

average SAR for both a homogeneous and a multilayered model of man, for E- and H-polarizations. The homogeneous results have been obtained using a combination of prolate spheroidal and cylindrical models [7].

The data presented in Fig. 6 suggest that the effect of layers in general is to change the SAR in the frequency range of 0.4–8 GHz in man-sized models. The enhancement of absorption at about 2 GHz and reduction at 5 GHz represent the greatest deviation from the homogeneous results. At frequencies below 400 MHz, the layers are so thin compared to a wavelength as to have a negligible effect, and at frequencies above 10 GHz the depth of penetration is so low that the transmitted power is all absorbed in the surface skin layer, which has the same permittivity as that of muscle material of the homogeneous model.

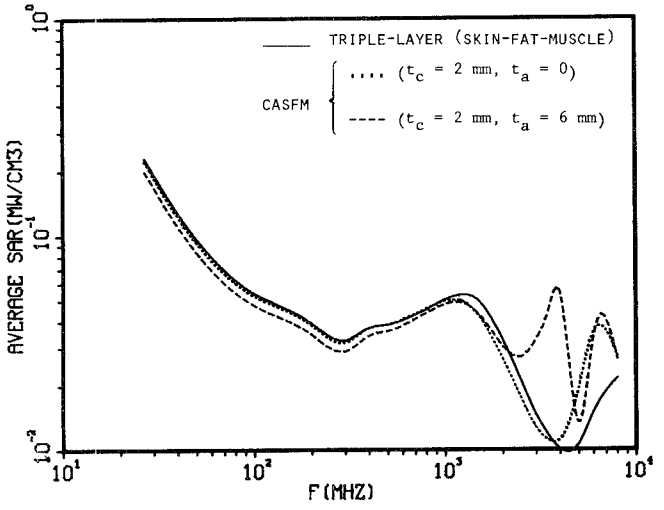

Fig. 7. Average SAR characteristics of the triple-layer cylindrical model of an average man with and without clothing, *E*-polarization. The incident power density is 1 mW/cm^2.

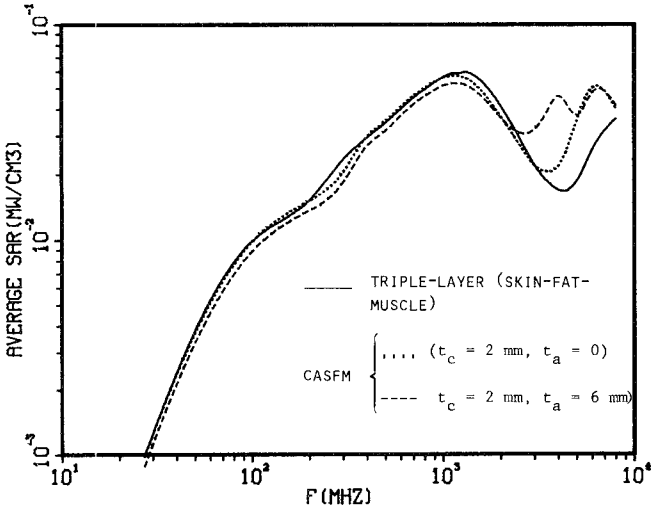

Fig. 8. Average SAR characteristics of the triple-layer cylindrical model of an average man with and without clothing, *H*-polarization. The incident power density is 1 mW/cm^2.

V. Absorption Effects Due to Clothing

The average SAR has been calculated for a multilayer cylindrical model of man consisting of clothing-air-skin-fat-muscle (CASFM). The underlying skin-fat-muscle cylinder is the same model as used in Figs. 2 and 3. Fig. 7 shows the average SAR as a function of frequency with air space as a parameter, along with the SAR for the basic triple-layered model, for *E*-polarization. In Fig. 7, t_c and t_a represent the thickness of clothing and air space, respectively. The complex permittivity of clothing is chosen to be $\epsilon = 10 - j5$ for all frequencies. The choice of this value is based on published data on the complex permittivity of wet clothing [10], [11] and also upon measurements in the 400–915-MHz frequency range of the dielectric constant and the conductivity of wet clothing (100-percent water content) made by the authors. Fig. 8 shows the average SAR as a function of frequency for the same model for *H*-polarization.

It is interesting to note that for frequencies below 2 GHz, the frequency dependence of the average SAR in the model with wet clothing remains the same as for the triple layer itself and the clothing has very little effect on the SAR. This result was expected because of the low dielectric constant and low-loss tangent of the wet clothing material compared to the high complex permittivity of the skin. However, for frequencies between 2 and 8 GHz, some secondary peaks can be seen in the average SAR value for the model with lossy clothing. The frequency of these secondary peaks depends on the thicknesses of the clothing and the air space, and also on the complex permittivity of the clothing. The results of SAR calculations for the model with dry clothing (with $\epsilon_c = 4.0$, a typical value for wool fibers in the low gigahertz range) show that the dry clothing has negligible effect on the SAR characteristics.

V. Conclusions

The absorption characteristics of multilayered cylindrical models of man exposed to perpendicularly incident EM plane waves have been investigated. Previous SAR calculations for homogeneous models of man have been modified to include the effects of layers on absorption. The calculated data presented in this paper lead to the following conclusions.

1) The effect of layers is generally to change the average SAR values in the frequency range of 0.4–8 GHz. The effects are not considerably large, since the greatest increase, which occurs at about 2 GHz, is approximately double that of the homogeneous model, and the greatest decrease, which occurs at about 5 GHz, is approximately half that of the homogeneous model.

2) The location of the layering resonance and the enhancement of the absorption due to layers are found to be almost identical for both planar and cylindrical models.

3) The frequency of the layering resonance is found to be independent of the polarization.

4) For given permittivities of the layers, the layering resonant frequency is inversely proportional to the thickness of the layers.

5) For frequencies below 2 GHz, the clothing has very little effect on the SAR value. However, for higher frequencies, some secondary peaks have been found in the average SAR values for the model with lossy clothing.

Acknowledgment

The authors wish to thank Dr. Te-Kao Wu for furnishing the computer program for calculation of the scattering coefficients.

References

[1] W. T. Joines and R. J. Spiegel, "Resonance absorption of microwaves by the human skull," *IEEE Trans. Biomed. Eng.*, vol. BME-21, pp. 46–48, Jan. 1974.

[2] C. M. Weil, "Absorption characteristics of multilayered sphere

models exposed to UHF/microwave radiation," *IEEE Trans. Biomed. Eng.*, vol. BME-22, pp. 468–476, Nov. 1975.
[3] P. W. Barber, O. P. Gandhi, M. J. Hagmann, and I. Chatterjee, "Electromagnetic absorption in a multilayered model of man," *IEEE Trans. Biomed. Eng.*, pp. 400–404, July 1979.
[4] H. Massoudi, C. H. Durney, and C. C. Johnson, "Geometrical optics and exact solutions for internal fields and SAR's in a cylindrical model of man as irradiated by an electromagnetic planewave," in *Abstracts of Scientific Papers, URSI Int. Symp. on the Biological Effects of the Electromagnetic Waves*, Airlie, VA, Oct. 30–Nov. 4, 1977, p. 49; also in special issue of *Radio Sci.* in press.
[5] H. E. Bussey and J. H. Richmond, "Scattering by a lossy dielectric circular cylindrical multilayer, numerical values," *IEEE Trans. Antennas Propagat.*, vol. AP-23, pp. 723–725, Sept. 1975.
[6] H. C. Van de Hulst, *Light Scattering by Small Particles*. New York: Wiley, 1957.
[7] C. H. Durney, C. C. Johnson, P. W. Barber, H. Massoudi, M. Iskander, S. J. Allen, and J. C. Mitchell, *Radiofrequency radiation dosimetry handbook: second edition*. Departments of Electrical Engineering and Bioengineering, University of Utah, Salt Lake City, 1978, (available from the authors).
[8] A. C. Eyeleshymer and D. M. Schoemaker, *A Cross-Section Anatomy*. New York: Appleton, 1911.
[9] D. J. Morton, *Manual of Human Cross Section Anatomy*. Baltimore, MD: Williams and Wilkins, 1944.
[10] W. E. Morton and J. W. S. Hearle, *Physical Properties of Textile Fibers*. London, England: William Heinemann, 1975.
[11] J. J. Windle and T. M. Shaw, "Dielectric properties of wool-water systems at 3000 and 9300 megacycles," *J. Chemical Phys.*, vol. 22, no. 10, pp. 1752–1757, Oct. 1954.

Computer-Aided Large-Signal Measurement of IMPATT-Diode Electronic Admittance

BARRY A. SYRETT, MEMBER, IEEE

Abstract—**A technique for the measurement of the large-signal electronic admittance of IMPATT diodes as a function of frequency and RF voltage level using the network analyzer is described. The method de-embeds the admittance of the active region of the device from the mounting and measurement circuitry without physical disturbance of the diode. The small series resistance of the diode at breakdown is included in the embedding network together with the mount and diode package parameters. The determination of transformation networks between the measurement port and the active chip through a simple calibration procedure, a knowledge of the diode admittance below breakdown, and computer-aided optimization constitute the de-embedding procedure. Experimental electronic admittance curves are given for a low-power (100-mW) silicon IMPATT diode in the frequency range 5.7–6.5 GHz and with RF voltage levels applied across the active chip in the range 0–24 V, with an estimated error of less than 20 percent (typically 5 percent) in admittance values.**

I. Introduction

LARGE-SIGNAL characterization of an IMPATT diode *in situ* is essential to the investigation of nonlinear phenomena occurring in IMPATT-diode amplifiers. A fundamental problem in these measurements is deembedding the active-chip electronic admittance Y_e from the passive packaging and mounting network with its many parasitic reactances. This paper describes a rapid accurate technique for the measurement of large-signal IMPATT-diode electronic admittance as a function of RF voltage level and frequency. The method combines and refines the features of several published small-signal measurement procedures and extends them into the large-signal region, viz., 1) the use of a network analyzer for rapidity of measurement [1]–[3], [5], 2) direct transformation of electronic admittance to device terminal admittance [3]–[5], 3) determination of the transformation network without physical disturbance of the diode and circuit [3]–[6], 4) computer reduction of measured data [1]–[6], and 5) accuracy enhancement by the use of an optimization routine in the calibration and measurement process [3]–[5]. The present method is more accurate than the large-signal technique of Young and Stephenson [7] which does not incorporate features 2)–5).

Manuscript received August 14, 1978; revised April 30, 1979. This work was supported by the National Research Council of Canada under operating grants.

The author was with the Department of Electrical Engineering, University of Alberta, Edmonton, Alta., Canada. He is now with the Department of Electronics, Carleton University, Ottawa, Ont., Canada.

II. Experimental Setup

A schematic diagram of the admittance measurement setup is shown in Fig. 1. The measurement technique allows the diode under test to be operated in a microwave cavity under typical operating conditions while the measurements are carried out. For present purposes, the IMPATT diode is end-mounted in a precision 50-Ω coaxial cavity with movable slug tuning, although other configurations are also suitable. Constant bias current is applied

0018-9480/79/1000-0830$00.75 ©1979 IEEE